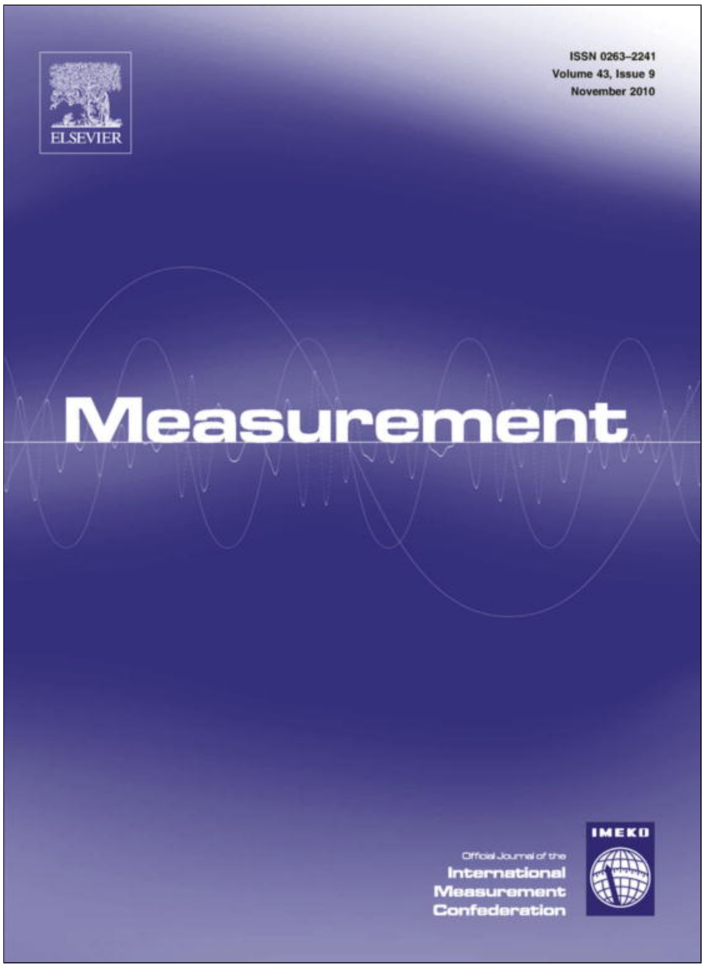
ELSEVIER
ISSN 0263-2241
Volume 43, Issue 9
November 2010
Measurement
Official Journal of the
International
Measurement
Confederation
IMEKO

Measurement 43 (2010) 1077–1089

Contents lists available at ScienceDirect

Measurement

journal homepage: www.elsevier.com/locate/measurement

Review

Critical remarks on the linearised and extended Kalman filters with geodetic navigation examples

Dah-Jing Jwo [a,*], Ta-Shun Cho [b]

[a] Department of Communications, Navigation and Control Engineering, National Taiwan Ocean University, 2 Peining Rd., Keelung 202-24, Taiwan
[b] Department of International Business Studies, National Chi Nan University, 1 University Rd., Puli, Nantou Hsien 545, Taiwan

ARTICLE INFO

Article history:
Received 11 August 2008
Received in revised form 10 February 2009
Accepted 26 May 2010
Available online 31 May 2010

Keywords:
Linearised Kalman filter
Extended Kalman filter
Total state estimate
Error state estimate
Navigation

ABSTRACT

The Kalman filter has been used in a wide variety of engineering applications. There are two typical forms in implementing the nonlinear Kalman filter in conjunction with linearisation trajectory for which calculation of Jacobian matrices is involved: the linearised Kalman filter (LKF) and the extended Kalman filter (EKF). This paper aims to serve as a tutorial to the readers for providing better understanding and correctly implementing the two forms of nonlinear filters. Some critical remarks useful in designing a nonlinear Kalman filter are pointed out. Linearisation of the trajectory for the LKF and EKF is discussed. Performance degradation due to linearisation error is illustrated. Divergence problem for the LKF is presented. Implementation practice for the LKF and the EKF via total state estimate in conjunction with the error state estimate (in which the state variables are incremental quantities) are provided. Discussion on increase of dynamic process noise to the estimation precision in LKF and EKF is involved. Clear description of the implementation algorithms is provided. The step-by-step procedure for performing the filters is provided accompanied with two geodetic navigation examples. The materials prepared in this paper can be modified for further development in various applications.

Contents

* Corresponding author. Tel.: +886 2 24622192x7209; fax: +886 2 24633492.
E-mail addresses: djjwo@mail.ntou.edu.tw (D.-J. Jwo), tashun@yahoo.com (T.-S. Cho).

0263-2241/$ - see front matter © 2010 Elsevier Ltd. All rights reserved.
doi:10.1016/j.measurement.2010.05.008

1. Introduction

The Kalman filter (KF) [1–6], commonly used in estimating the system state variables and suppress the measurement noise, has been recognized as one of the most powerful state estimation techniques. The Kalman filter is attractive because it has been shown to be able to minimize the variance of the estimation mean square error (MSE). For nonlinear dynamics and/or nonlinear measurement relationships, the problem of estimating the state variables of the nonlinear systems may be solved using the nonlinear version of the Kalman filter. Both the Kalman filter and its nonlinear version, linearised Kalman filter and extended Kalman filter, has been successfully applied in engineering applications, e.g., in the areas of aerospace, marine navigation, radar target tracking, control systems, manufacturing, and many others. In addition to engineering applications, the KF can also be employed for time series analysis, e.g. to predict stock prices or currency exchange rate. Studying the operation of the Kalman filter leads to an appreciation of the inter-disciplinary nature of system engineering.

Theoretical-oriented paper on error self-correction in dynamic systems using the innovation sequence was presented by Hajiyev [7]. Investigators have presented several Kalman filter related applications in the fields of navigation, such as GPS receiver position and velocity determination [8], inertial navigation alignment [9], attitude determination [10,11], and integrated navigation system design [12,13]. Shmaliy et al. [8] proposed a thinning algorithm for real-time unbiased finite impulse response (FIR) estimation of the local clock time interval error (TIE) model, and compared to that of three state Kalman filter, in terms of the Allan deviation and precision time protocol deviation. Ali and Ushaq [9] presented a reliable in-motion alignment scheme for a low-cost strapdown inertial navigation system (SINS) using a consistent and robust Kalman filter structure, by integrating SINS data with the Global Positioning System (GPS) by using some form of measurement matching method. Wang and Jin [10] developed a mini-type and portable attitude measurement system used in self-propelled model trials for the ships, which involves complete design, calibration and alignment procedure based on the robust Kalman filtering. Zhu et al. [11] investigated the linear fusion algorithm for attitude determination using low-cost MEMS-based sensors. Bogatin et al. [12] assessed the efficiency of the linear Kalman filter as a method for the estimation of kinematic process observed with electronic tacheometer. In their contribution, the efficiency of the three-dimensional linear Kalman filter model, in combination with the law on transfer of variances and covariances, is controlled using a known reference trajectory and statistical tests. Salahshoor et al. [13] presents an integrated design framework to utilize multi-sensor data fusion techniques for process monitoring enhancement to detect and diagnose sensor and process faults. Two different distributed and centralized architectures were presented for integrating the multi-sensor data based on extended Kalman filter (EKF) data fusion algorithm and developed a new adaptive modified EKF (AMEKF) algorithm to prevent the filter divergence.

Some important measurement and instrumentation science and technology related issues have been presented [14–17]. For example, an analytical review of the development of measurement and instrumentation science is given by Finkelstein [14]. An overview on modelling in measurement and instrumentation science can be found in [15]. The basic notions of measurement science are overviewed in [16]. Graphic-based representations for measurement science are given in [17], where a general scheme of measurement was proposed that emphasizes the key role of measured reconstruction. Although some other nonlinear filters have been proposed, the nonlinear version of Kalman filter still plays the vital role in geodetic navigation as the sensor fusion and data processing tool. As a popular tool in the filed of measurement science and technology, a lesson that covers the critical issues on the two forms of nonlinear Kalman filters are of importance. The two approaches to Kalman filter approximations for nonlinear problems yield different implementation equations. Two of the popular forms are the linearised Kalman filter (LKF) and the extended Kalman filters (EKF), which have become standard techniques used in a number of nonlinear estimation applications. Implementation of the nonlinear Kalman filter is not as simple as that of the linear Kalman filter. To serve as a tutorial to the readers for providing better understanding and correctly implementing the two forms of nonlinear filters, useful information on several practical while critical issues regarding the linearised and extended Kalman filters will be conveyed.

The LKF and EKF approximate (linearise) the nonlinear functions in the state dynamic and measurement model. The EKF is linearised about the current estimate of the state, whereas the LKF utilizes a precomputed nominal trajectory. From the theoretical point of view, the LKF and EKF are both suboptimal since they are propagated analytically through the first-order linearisation of the nonlinear system. As the deviation between actual trajectory and nominal one increases, the significance of the higher order terms (*hot's*) in the Taylor series expansion of the trajectory also increases. The LKF approach generally has more efficient real-time implementation, but it is less robust against nonlinear approximation errors than the EKF. The real-time implementation of the LKF can be made more efficient by precomputing the measurement sensitivities, state transition matrices, and Kalman gains. Nevertheless, the problem with linearisation about the nominal trajectory is that the deviation between actual trajectory and nominal one tends to increase with time. The series approximations in the LKF/EKF algorithm can lead to poor representations of the nonlinear functions and probability distributions of interest. The linearisation can lead into large errors in the true posterior mean and covariance of the transformed random variable, which may yield divergence of the filter. In the average, the EKF generally exhibits better robustness in comparison with LKF since EKF uses linear approximation over smaller ranges of state space.

There are two basic ways for implementing the EKF: total state space formulation (also referred to as the direct formulation) and error state space formulation (also referred to as the indirect formulation). In the total state space formulation, the system is essentially dominated by the vehicle motion. On the other hand, the measurement in the error state space formulation is made up entirely of system errors and is almost independent of vehicle motions. Content of discussion covers the performance degradation due to uncertainty in reference trajectory, implementation practice for the LKF and the EKF via total state estimate in conjunction with the error state estimate, clear description of the algorithms and step-by-step explanation of the implementation procedures, and summary of algorithm. The materials presented in this contribution are beneficial to the nonlinear Kalman filter designers. The informative materials can be employed as guidelines for developing a suitable nonlinear Kalman filter design.

This paper is organized as follows. In Section 2, suboptimal nonlinear Kalman filter are discussed, which covers the critical characteristics of linearised Kalman filter and the extended Kalman filter, the connection between total state estimate and the error state estimate of EKF, and clear presentation of the associated algorithms. Examples for geodetic navigation will be employed for illustration. In Section 3, the example is focused on the example of nominal trajectory unavailable. The illustrative example focused on the example of nominal trajectory available is discussed in Section 4. The conclusion is given in Section 5.

2. Suboptimal nonlinear Kalman filter

Some of the materials covered in this section are closely related to the contents in books by Brown and Hwang [3], and Grewal and Andrews [5]. However, some in deep exploration accompanied with informative implementation algorithms is presented.

Both the LKF and the EKF are recognized as the nonlinear versions of KF, dealing with the case governed by the nonlinear stochastic differential equations. The two basic ways of linearising the nonlinear KF problem are (1) linearised Kalman filter (LKF, also known as the perturbation Kalman filter), which linearises about some nominal trajectory in state space that does not depend on the measurement data; (2) extended Kalman filter (EKF), which linearises about a trajectory that is continually updated with the state estimates. From the view points of Taylor's series expansion, both LKF and EKF are suboptimal nonlinear filters since both filters achieve the first-order precision (by neglecting the higher order terms).

Assuming the process to be estimated and the associated measurement relationship may be written in the form:

$$\mathbf{x}_{k+1} = \mathbf{f}(\mathbf{x}_k, k) + \mathbf{w}_k \tag{1a}$$

$$\mathbf{z}_k = \mathbf{h}(\mathbf{x}_k, k) + \mathbf{v}_k \tag{1b}$$

where $\mathbf{f}$ and $\mathbf{h}$ are known functions, the state vector $\mathbf{x}_k \in \Re^n$, process noise vector $\mathbf{w}_k \in \Re^n$, measurement vector $\mathbf{z}_k \in \Re^m$, and measurement noise vector $\mathbf{v}_k \in \Re^m$.

Both the vectors $\mathbf{w}_k$ and $\mathbf{v}_k$ are zero mean Gaussian white sequences having zero crosscorrelation with each other:

$$\mathbf{E}[\mathbf{w}_k\mathbf{w}_i^{\mathrm{T}}] = \begin{cases} \mathbf{Q}_k, & i = k \\ 0, & i \neq k \end{cases} \; \mathbf{E}[\mathbf{v}_k\mathbf{v}_i^{\mathrm{T}}] = \begin{cases} \mathbf{R}_k, & i = k \\ 0, & i \neq k \end{cases}; \; \mathbf{E}[\mathbf{w}_k\mathbf{v}_i^{\mathrm{T}}] = \mathbf{0} \quad \text{for all } i \text{ and } k \tag{2}$$

where $\mathbf{E}[\cdot]$ represents expectation, and superscript "T" denotes matrix transpose, $\mathbf{Q}_k$ is the process noise covariance matrix and $\mathbf{R}_k$ is the measurement noise covariance matrix.

If $\mathbf{f}$ and $\mathbf{h}$ are continuously differentiable infinitely often, then the influence of the perturbations on the trajectory can be represented by a Taylor series expansion about the nominal trajectory. The likely magnitudes of the perturbations are determined by the variances of the variates involved. One can obtain a good approximation by ignoring terms beyond some order if these perturbations are sufficiently small relative to the higher order terms of the expansion.

2.1. The linearised Kalman Filter

Nonlinearity may enter into the problem either in the dynamics of the process or in the measurement relationship. $\mathbf{x}_k = \mathbf{x}_k^* + \delta\mathbf{x}_k$, then

$$\mathbf{x}_{k+1} = \mathbf{f}(\mathbf{x}_k^* + \delta\mathbf{x}_k, k) + \mathbf{w}_k \tag{3a}$$

$$\mathbf{z}_k = \mathbf{h}(\mathbf{x}_k^* + \delta\mathbf{x}_k, k) + \mathbf{v}_k \tag{3b}$$

where δ denotes perturbations from the nominal.

Assuming $\delta\mathbf{x}$ is small and approximating $\mathbf{f}$ functions with Taylor's series expansions leading the result as

$$\mathbf{x}_{k+1} = \mathbf{f}(\mathbf{x}_k, k) = \mathbf{f}(\mathbf{x}_k^*, k) + \left[\frac{\partial \mathbf{f}(\mathbf{x}_k, k)}{\partial \mathbf{x}}\right]\bigg|_{\mathbf{x}=\mathbf{x}_k^*} \cdot \delta\mathbf{x}_k + hot\text{'s}$$

It is customary to choose the nominal trajectory $\mathbf{x}_k^*$ to satisfy the deterministic differential equation $\mathbf{x}_{k+1}^* = \mathbf{f}(\mathbf{x}_k^*, k)$; therefore, we have

$$[\mathbf{x}_{k+1} - \mathbf{x}_{k+1}^*] = \left[\frac{\partial \mathbf{f}(\mathbf{x}_k, k)}{\partial \mathbf{x}}\right]\bigg|_{\mathbf{x}=\mathbf{x}_k^*} \cdot \delta\mathbf{x}_k + hot\text{'s}$$

Form $\mathbf{z}_k = \mathbf{h}(\mathbf{x}_k^* + \delta\mathbf{x}_k, k) + \mathbf{v}_k$, approximating $\mathbf{h}$ functions with Taylor's series expansions leading the result as

$$[\mathbf{z}_k - \mathbf{h}(\mathbf{x}_k^*, k)] = \left[\frac{\partial \mathbf{h}(\mathbf{x}_k, k)}{\partial \mathbf{x}}\right]\bigg|_{\mathbf{x}=\mathbf{x}_k^*} \cdot \delta\mathbf{x}_k + hot\text{'s}$$

By definition $\delta\mathbf{x}_{k+1} = \mathbf{x}_{k+1} - \mathbf{x}_{k+1}^*$ and $\delta\mathbf{z}_k = \mathbf{z}_k - \mathbf{h}(\mathbf{x}_k^*, k)$, and retaining only first-order terms leads to the linearised models:

$$\text{linearised dynamics equation}: \quad \delta\mathbf{x}_{k+1} = \boldsymbol{\Phi}_k\delta\mathbf{x}_k + \mathbf{w}_k \tag{4a}$$

$$\text{linearised measurement equation}: \quad \delta\mathbf{z}_k = \mathbf{H}_k\delta\mathbf{x}_k + \mathbf{v}_k \tag{4b}$$

In this case, the "measurement" here represents the total measurement minus the predicted one. The $\boldsymbol{\Phi}_k$ and $\mathbf{H}_k$ matrices are obtained by evaluating the partial derivative matrices along the nominal trajectory:

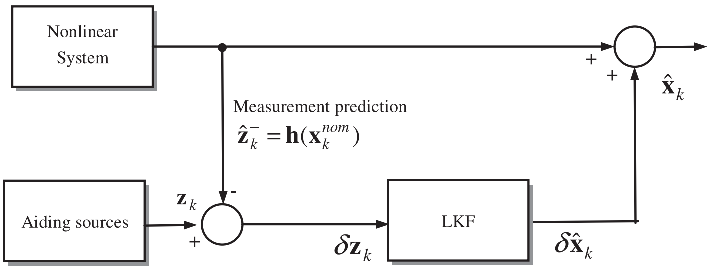

Fig. 1. Configuration of the LKF (error sate estimate formulation).

Table 1
Summary of LKF equations (error state formulation).

– Nonlinear model:
  Nonlinear nominal trajectory model: $\mathbf{x}_{k+1}^{nom} = \mathbf{f}(\mathbf{x}_k^{nom}, k)$
  Nonlinear measurement model: $\mathbf{z}_k = \mathbf{h}(\mathbf{x}_k, k) + \mathbf{v}_k$

– Linearised perturbed trajectory model:
  Linearised dynamic model: $\delta\mathbf{x}_{k+1} = [\frac{\partial \mathbf{f}}{\partial \mathbf{x}}]|_{\mathbf{x}=\mathbf{x}_k^{nom}} \delta\mathbf{x}_k + \mathbf{w}_k$
  Linearised measurement model: $\delta\mathbf{z}_k = [\frac{\partial \mathbf{h}}{\partial \mathbf{x}}]|_{\mathbf{x}=\mathbf{x}_k^{nom}} \delta\mathbf{x}_k + \mathbf{v}_k$

$$\mathbf{K}_k = \mathbf{P}_k^- \mathbf{H}_k^T [\mathbf{H}_k \mathbf{P}_k^- \mathbf{H}_k^T + \mathbf{R}_k]^{-1} \quad \text{(T1)}$$

$$\delta\hat{\mathbf{x}}_k = \delta\hat{\mathbf{x}}_k^- + \mathbf{K}_k[\delta\mathbf{z}_k - \mathbf{H}_k \delta\hat{\mathbf{x}}_k^-] \quad \text{(T2)}$$

$$\hat{\mathbf{x}}_k = \mathbf{x}_k^{nom} + \delta\hat{\mathbf{x}}_k \quad \text{(T3)}$$

$$\mathbf{P}_k = [\mathbf{I} - \mathbf{K}_k \mathbf{H}_k]\mathbf{P}_k^- \quad \text{(T4)}$$

$$\delta\hat{\mathbf{x}}_{k+1}^- = \boldsymbol{\Phi}_k \delta\hat{\mathbf{x}}_k \quad \text{(T5)}$$

$$\mathbf{P}_{k+1}^- = \boldsymbol{\Phi}_k \mathbf{P}_k \boldsymbol{\Phi}_k^T + \mathbf{Q}_k \quad \text{(T6)}$$

where the linear approximation equations for system and measurement matrices are obtained through the relations

$$\boldsymbol{\Phi}_k \approx \left[\frac{\partial \mathbf{f}}{\partial \mathbf{x}}\right]\Big|_{\mathbf{x}=\mathbf{x}_k^{nom}}; \quad \mathbf{H}_k \approx \left[\frac{\partial \mathbf{h}}{\partial \mathbf{x}}\right]\Big|_{\mathbf{x}=\mathbf{x}_k^{nom}} \quad \text{(T7)}$$

and $\delta\mathbf{x}_k = \mathbf{x}_k - \mathbf{x}_k^{nom}$, $\delta\mathbf{z}_k = \mathbf{z}_k - \mathbf{h}(\mathbf{x}_k^{nom}, k)$.

$$\boldsymbol{\Phi}_k = \left[\frac{\partial \mathbf{f}}{\partial \mathbf{x}}\right]\Big|_{\mathbf{x}=\mathbf{x}_k^*} = \left.\begin{bmatrix} \frac{\partial f_1}{\partial x_1} & \frac{\partial f_1}{\partial x_2} & \cdots & \frac{\partial f_1}{\partial x_m} \\ \frac{\partial f_2}{\partial x_1} & \frac{\partial f_2}{\partial x_2} & \cdots & \frac{\partial f_2}{\partial x_m} \\ \vdots & \vdots & \ddots & \vdots \\ \frac{\partial f_m}{\partial x_1} & \frac{\partial f_m}{\partial x_2} & \cdots & \frac{\partial f_m}{\partial x_m} \end{bmatrix}\right|_{\mathbf{x}=\mathbf{x}_k^*};$$

$$\mathbf{H}_k = \left[\frac{\partial \mathbf{h}}{\partial \mathbf{x}}\right]\Big|_{\mathbf{x}=\mathbf{x}_k^*} = \left.\begin{bmatrix} \frac{\partial h_1}{\partial x_1} & \frac{\partial h_1}{\partial x_2} & \cdots & \frac{\partial h_1}{\partial x_m} \\ \frac{\partial h_2}{\partial x_1} & \frac{\partial h_2}{\partial x_2} & \cdots & \frac{\partial h_2}{\partial x_m} \\ \vdots & \vdots & \ddots & \vdots \\ \frac{\partial h_m}{\partial x_1} & \frac{\partial h_m}{\partial x_2} & \cdots & \frac{\partial h_m}{\partial x_m} \end{bmatrix}\right|_{\mathbf{x}=\mathbf{x}_k^*} \quad (5)$$

The LKF is computationally advantageous as compared to the EKF, but it can also suffer from large magnitude errors if the true and nominal trajectories differ significantly [3]. The feedforward error state space Kalman filter is an example of this configuration. Fig. 1 is the configuration of the LKF (implementation via error sate formulation). Table 1 summarizes the LKF equations.

The nonlinear functions in dynamic and measurement models are approximated by the first term in their Taylor series expansion. They are based on the assumption that local linearisation of the above equations may be a sufficient description of nonlinearity. Also, the measurement presented to the linearised filter is the total measurement minus the predicted measurement based on the nominal position $\mathbf{x}_k^{nom}$ (i.e., $\delta\mathbf{z}_k = \mathbf{z}_k - \mathbf{h}(\mathbf{x}_k^{nom}, k)$). The basic concept is that the linearised filter is always estimating the incremental (delta) quantities, and then the total quantities are reconstructed by adding the incremental estimate to the nominal part.

2.2. The extended Kalman filter: error state estimate configuration

A simple effective remedy for the deviation problem is to replace the nominal trajectory with the estimated trajectory. That is, to evaluate the Taylor series expansion about the estimated trajectory. The extended Kalman filter is similar to a linearised Kalman filter except that the linearisation takes place about the filter's estimated trajectory, rather than a precomputed nominal trajectory. The only modification required is to replace $\mathbf{x}_k^{nom}$ by $\hat{\mathbf{x}}_k^-$ in the evaluations of partial derivatives. That is, the partial derivatives are evaluated along a trajectory that has been updated with the filter's estimates; which depend on the measurements, and therefore the filter gain sequence will depend on the sample measurement sequence. If the problem is sufficiently observable (as evidenced by the covariance of estimation uncertainty), then the deviations between the estimated trajectory (along which the expansion is made) and the actual trajectory will remain sufficiently small that the linearisation assumption is valid.

The problem with linearisation about the nominal trajectory is that the deviation of the actual trajectory from the nominal trajectory tends to increase with time. The basic idea of the EKF is to relinearise about each estimate as soon as it has been computed. When a new state estimate is made, a better reference state trajectory is then incorporated into the estimation process. Consequently, one enhances the validity of the assumption that deviations from the reference (nominal) trajectory are small enough to allow linear perturbation techniques to be employed with adequate results. The extended Kalman filter is a somewhat riskier filter than the regular linearised filter. It may be better on the average than the linearised filter, but it may also be more likely to diverge in some unusual situations.

There are two configurations in the EKF implementation [3,5,6]: error state estimate vs. total state estimate. The principal drawback to this approach is that it tends to in-

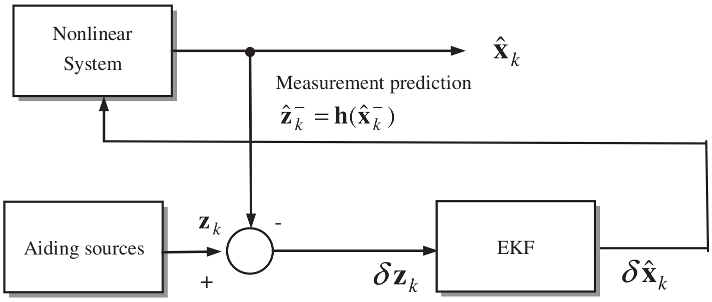

Fig. 2. Configuration of the EKF with error sate estimate.

Table 2
Summary of EKF equations – error state formulation.

– Nonlinear model:
Dynamic model: $\mathbf{x}_{k+1} = \mathbf{f}(\mathbf{x}_k, k) + \mathbf{w}_k$
Measurement model: $\mathbf{z}_k = \mathbf{h}(\mathbf{x}_k) + \mathbf{v}_k$

– Linearised model:
Linearised dynamic model: $\delta\mathbf{x}_{k+1} = [\frac{\partial \mathbf{f}}{\partial \mathbf{x}}]|_{\mathbf{x}=\hat{\mathbf{x}}_k^-} \delta\mathbf{x}_k + \mathbf{w}_k$
Linearised measurement model: $\delta\mathbf{z}_k = [\frac{\partial \mathbf{h}}{\partial \mathbf{x}}]|_{\mathbf{x}=\hat{\mathbf{x}}_k^-} \delta\mathbf{x}_k + \mathbf{v}_k$

$\delta\mathbf{z}_k = \mathbf{z}_k - \mathbf{h}(\hat{\mathbf{x}}_k^-, k)$

$$\mathbf{K}_k = \mathbf{P}_k^-\mathbf{H}_k^T[\mathbf{H}_k\mathbf{P}_k^-\mathbf{H}_k^T + \mathbf{R}_k]^{-1} \quad \text{(T8)}$$

$$\delta\hat{\mathbf{x}}_k = \delta\hat{\mathbf{x}}_k^- + \mathbf{K}_k[\delta\mathbf{z}_k - \mathbf{H}_k\delta\hat{\mathbf{x}}_k^-] \quad \text{(T9)}$$

$$\hat{\mathbf{x}}_k = \hat{\mathbf{x}}_k^- + \delta\hat{\mathbf{x}}_k \quad \text{(T10)}$$

$$\mathbf{P}_k = [\mathbf{I} - \mathbf{K}_k\mathbf{H}_k]\mathbf{P}_k^- \quad \text{(T11)}$$

$$\hat{\mathbf{x}}_{k+1}^- = \mathbf{f}(\hat{\mathbf{x}}_k, k) \quad \text{(T12)}$$

$$\delta\hat{\mathbf{x}}_{k+1}^- = \mathbf{0} \quad \text{(T13)}$$

$$\mathbf{P}_{k+1}^- = \boldsymbol{\Phi}_k\mathbf{P}_k\boldsymbol{\Phi}_k^T + \mathbf{Q}_k \quad \text{(T14)}$$

where the linear approximation equations for system and measurement matrices are obtained through the relations

$$\boldsymbol{\Phi}_k = \left[\frac{\partial \mathbf{f}}{\partial \mathbf{x}}\right]\bigg|_{\mathbf{x}=\hat{\mathbf{x}}_k^-}; \quad \mathbf{H}_k = \left[\frac{\partial \mathbf{h}}{\partial \mathbf{x}}\right]\bigg|_{\mathbf{x}=\hat{\mathbf{x}}_k^-} \quad \text{(T15)}$$

crease the real-time computational burden. The off-line computation is not possible for the EKF state estimates. Fig. 2 presents the configuration of the EKF implementation with error sate estimate. Table 2 summarizes the EKF equations via error state formulation.

For the configuration of the EKF with error state space estimate, several differences should be noticed.

(1) $\hat{\mathbf{x}}_k = \hat{\mathbf{x}}_k^- + \delta\hat{\mathbf{x}}_k$. The total state estimate vector ($\hat{\mathbf{x}}_k$) is formed by summing the nominal ($\hat{\mathbf{x}}_k^-$) with the estimated incremental (delta) quantities ($\delta\hat{\mathbf{x}}_k$). The result is consistent with the result given in Section 2.3, the total state estimate configuration.
(2) $\hat{\mathbf{x}}_{k+1}^- = \mathbf{f}(\hat{\mathbf{x}}_k, k)$. For an extended Kalman filter, the current estimate is used to form the next nominal point (i.e., the next point around which the linearisation will take place).
(3) $\delta\hat{\mathbf{x}}_{k+1}^- = \mathbf{0}$. For an EKF, the state prediction is zeros since after the update is made in the EKF, the incremental quantities $\delta\hat{\mathbf{x}}_k$ is reduced to zero. The projection of $\delta\hat{\mathbf{x}}_k$ to the next step is trivial. The only nontrivial projection is to project $\hat{\mathbf{x}}_k$ to $\hat{\mathbf{x}}_{k+1}^-$.

2.3. The extended Kalman filter: total state estimate configuration

The basic state variables in a LKF are incremental (delta) quantities, rather than the total quantities. However, in an EKF it is accessible to keep track of the total estimates rather than the incremental ones. The basic linearised measurement equation for the EKF can be written as

$$\mathbf{z}_k - \mathbf{h}(\hat{\mathbf{x}}_k^-, k) = \mathbf{H}_k\delta\mathbf{x}_k + \mathbf{v}_k \quad (6)$$

Note that when working with incremental state variables, the measurement presented to the Kalman filter is $\mathbf{z}_k - \mathbf{h}(\hat{\mathbf{x}}_k^-, k)$ rather than the total measurement (nonlinear) $\mathbf{z}_k$. Consider the incremental estimate update equation at step k

$$\delta\hat{\mathbf{x}}_k = \delta\hat{\mathbf{x}}_k^- + \mathbf{K}_k[\mathbf{z}_k - \mathbf{h}(\hat{\mathbf{x}}_k^-, k) - \mathbf{H}_k\delta\hat{\mathbf{x}}_k^-] \quad (7)$$

in which the measurement residual is written as $\delta\mathbf{z}_k = \mathbf{z}_k - \mathbf{h}(\hat{\mathbf{x}}_k^-, k)$ and the predictive estimate of the measurement is the sum of $\mathbf{h}(\hat{\mathbf{x}}_k^-, k)$ and $\mathbf{H}_k\delta\hat{\mathbf{x}}_k^-$. This is the noisy measurement minus the predictive measurement based on the corrected trajectory rather than the nominal one.

Adding $\hat{\mathbf{x}}_k^-$ to both sides of the update equation leads to:

$$\hat{\mathbf{x}}_k^- + \delta\hat{\mathbf{x}}_k = \hat{\mathbf{x}}_k^- + \delta\hat{\mathbf{x}}_k^- + \mathbf{K}_k[\mathbf{z}_k - \hat{\mathbf{z}}_k^-]$$

and finally

$$\hat{\mathbf{x}}_k = \hat{\mathbf{x}}_k^- + \mathbf{K}_k[\mathbf{z}_k - \hat{\mathbf{z}}_k^-] \quad (8)$$

which is the estimate update equation written in terms of total rather than incremental quantities. It simply says that the *a priori* estimate is corrected by adding the measurement residual appropriately weighted by the Kalman gain matrix $\mathbf{K}_k$. After the update is made in the extended Kalman filter, the incremental quantity is reduced to zero and the projection of $\delta\hat{\mathbf{x}}_k^-$ to the next step is then trivial. The only nontrivial projection is to project $\hat{\mathbf{x}}_k$ to $\hat{\mathbf{x}}_{k+1}^-$, through the nonlinear dynamics: $\hat{\mathbf{x}}_{k+1}^- = \mathbf{f}(\hat{\mathbf{x}}_k, k)$. Notice that the additive white-noise forcing function $\mathbf{w}_k$ is zero in the projection step. Once $\hat{\mathbf{x}}_{k+1}^-$ is determined, the predictive measurement $\hat{\mathbf{z}}_{k+1}^-$ can be formed as $\mathbf{h}(\hat{\mathbf{x}}_{k+1}^-, k+1)$, and the measurement residual at $k+1$ is formed as the differ-

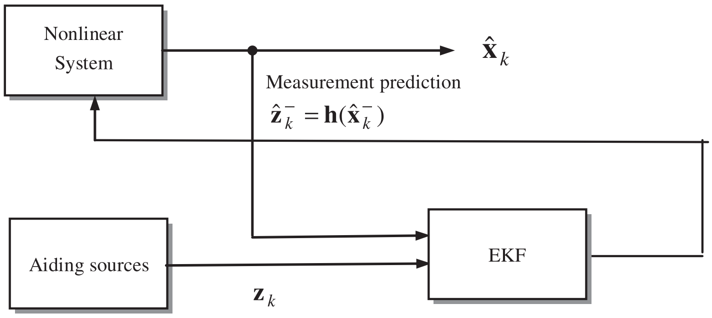

Fig. 3. Configuration of the EKF with total sate estimate.

Table 3
Summary of EKF equations - total state formulation.

– Nonlinear model
Nonlinear dynamic model: $\mathbf{x}_{k+1} = \mathbf{f}(\mathbf{x}_k, k) + \mathbf{w}_k$
Nonlinear measurement model: $\mathbf{z}_k = \mathbf{h}(\mathbf{x}_k, k) + \mathbf{v}_k$

$$\mathbf{K}_k = \mathbf{P}_k^- \mathbf{H}_k^T [\mathbf{H}_k \mathbf{P}_k^- \mathbf{H}_k^T + \mathbf{R}_k]^{-1} \quad \text{(T16)}$$

$$\hat{\mathbf{x}}_k = \hat{\mathbf{x}}_k^- + \mathbf{K}_k [\mathbf{z}_k - \hat{\mathbf{z}}_k^-] \quad \text{(T17)}$$

$$\mathbf{P}_k = [\mathbf{I} - \mathbf{K}_k \mathbf{H}_k] \mathbf{P}_k^- \quad \text{(T18)}$$

$$\hat{\mathbf{x}}_{k+1}^- = \mathbf{f}(\hat{\mathbf{x}}_k, k) \quad \text{(T19)}$$

$$\mathbf{P}_{k+1}^- = \boldsymbol{\Phi}_k \mathbf{P}_k \boldsymbol{\Phi}_k^T + \mathbf{Q}_k \quad \text{(T20)}$$

where the linear approximation equations for system and measurement matrices are obtained through the relations

$$\boldsymbol{\Phi}_k = \left.\frac{\partial \mathbf{f}_k}{\partial \mathbf{x}}\right|_{\mathbf{x}=\hat{\mathbf{x}}_k^-}; \quad \mathbf{H}_k = \left.\frac{\partial \mathbf{h}_k}{\partial \mathbf{x}}\right|_{\mathbf{x}=\hat{\mathbf{x}}_k^-} \quad \text{(T21)}$$

and $\hat{\mathbf{z}}_k^- = \mathbf{h}(\hat{\mathbf{x}}_k^-, k)$

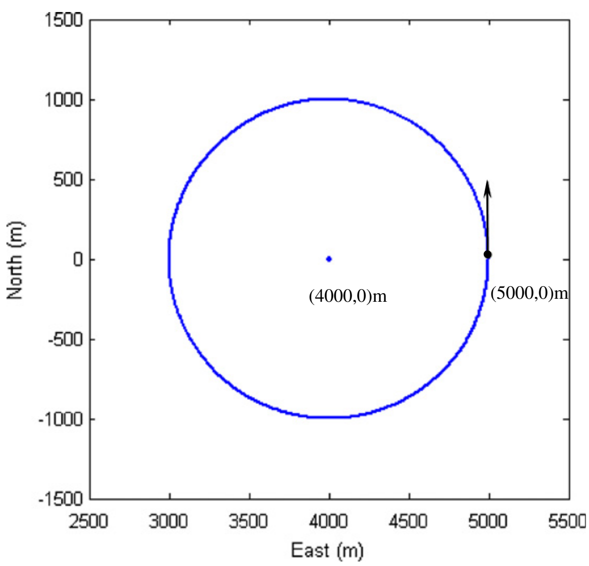

Fig. 4. Reference East–North trajectory for the DME navigation example.

ence $(\mathbf{z}_{k+1} - \hat{\mathbf{z}}_{k+1}^-)$. The filter is then ready to go through another recursive loop. Fig. 3 is the configuration of the EKF with total sate estimate. Table 3 summarizes the EKF equations via total state formulation.

3. Illustrative example – nominal trajectory in not available

Illustrative examples are provided. Two EKF formulations, i.e., total state estimate and error state estimate are provided. The two architectures yield the same results and therefore only one set of results is provided. The performance of the LKF will be degraded significantly. The situation is illustrated by the following examples.

The scenario for simulation is as follow. The true trajectory is assumed to move along a circle trajectory with a radius of 1 km, as shown in Fig. 4, is selected for simulation. The location of the origin is at (4000,0) m location in the local tangent ENU frame. The experiment was conducted on a simulated vehicle trajectory originating from the position of (5000,0) m location. The user was simulated to move in the counter-clockwise direction, at 226 km/h speed (62.832 m/s). The vehicle finally completes a circle movement within the simulation period. Navigation solutions were computed every 0.1 s, consequently, there are 1000 epochs recorded. The electronic navigation system that uses the noisy measurement of range from the vehicle to a known location as basic observable is the distance-measuring equipment (DME). It is usually assumed that the coordinates of the DME stations are known, and the aircraft coordinates are to be estimated. In this example, there are three ranging sources coming from three DME stations, which are located at the following positions: DME1 = (7000, −3000) m, DME2 = (3500, 5000) m, DME3 = (1000, −3000) m.

The basic differential equations of motion in the east (e) and north (n) directions are $\ddot{l}_e = 0 + u_e$ $\ddot{l}_n = 0 + u_n$.

The dynamical equations are seen to be linear in this case, so the differential equations for the incremental (delta) quantities are the same as for the total state variables l_e and l_n, that is

$$\delta\ddot{l}_e = u_e$$

$$\delta\ddot{l}_n = u_n$$

Defining the filter state variables in terms of the incremental positions and velocities:

$$x_1 = \delta l_e, \quad x_2 = \delta v_e$$

$$x_3 = \delta l_n, \quad x_4 = \delta v_n$$

the state equations are

$$\begin{bmatrix} \dot{x}_1 \\ \dot{x}_2 \\ \dot{x}_3 \\ \dot{x}_4 \end{bmatrix} = \begin{bmatrix} 0 & 1 & 0 & 0 \\ 0 & 0 & 0 & 0 \\ 0 & 0 & 0 & 1 \\ 0 & 0 & 0 & 0 \end{bmatrix} \begin{bmatrix} x_1 \\ x_2 \\ x_3 \\ x_4 \end{bmatrix} + \begin{bmatrix} 0 \\ u_e \\ 0 \\ u_n \end{bmatrix}$$

The state variables are driven by the white-noise processes u_e and u_n.

Assuming that three simultaneous range measurements are available, the three measurement equations in terms of l_e and l_n have the form

$$z_i = \sqrt{(l_e - a_i)^2 + (l_n - b_i)^2} + v_i, \quad i = 1 \ldots m$$

where v_i are additive white measurement noises. It can be seen that the connection between the observables (z_i) and the quantities to be estimated (l_e and l_n) is nonlinear. By assuming that an approximate nominal position is known at the time of the measurement, and that the locations of the three DME stations are known exactly, the $\mathbf{H}_k$ matrix can be found to be

$$\mathbf{H}_k = \frac{\partial \mathbf{h}}{\partial \mathbf{x}} = \begin{bmatrix} h_{11} & 0 & h_{13} & 0 \\ h_{21} & 0 & h_{23} & 0 \\ \vdots & \vdots & \vdots & \vdots \\ h_{n1} & 0 & h_{n3} & 0 \end{bmatrix}$$

where

$$h_{i1} = \frac{(l_e - a_i)}{\sqrt{(l_e - a_i)^2 + (l_n - b_i)^2}};$$

$$h_{i3} = \frac{(l_n - b_i)}{\sqrt{(l_e - a_i)^2 + (l_n - b_i)^2}}$$

are the direction cosine matrix elements. The nominal aircraft position will change with each step of the recursive process, so the terms of $\mathbf{H}_k$ are time-variable and must be recomputed with each recursive step.

In this example it is assumed that the aircraft and the three DME stations are all in a horizontal plane as shown in Fig. 4. The process noise characteristics is given by $u_e \sim N(0, q_e)$; $u_n \sim N(0, q_n)$. These spectral amplitudes are used to establish the $\mathbf{Q}_k$ matrix:

$$\mathbf{Q}_k = \begin{bmatrix} \frac{\Delta t^3}{3} q_e & \frac{\Delta t^2}{2} q_e & 0 & 0 \\ \frac{\Delta t^2}{2} q_e & \Delta t \cdot q_e & 0 & 0 \\ 0 & 0 & \frac{\Delta t^3}{3} q_n & \frac{\Delta t^2}{2} q_n \\ 0 & 0 & \frac{\Delta t^2}{2} q_n & \Delta t \cdot q_n \end{bmatrix}$$

In practical design, the power spectral density (PSD) values of the process noise should be properly tuned to reflect the vehicle dynamical profile. For straight and level flight, a small $\mathbf{Q}_k$ is appropriate. For turns or high dynamics, a larger $\mathbf{Q}_k$ should be used.

3.1. LKF performance

Performance based on three cases of nominal trajectories is discussed.

– *Case A:* Reference trajectory is given by the actual trajectory (For demonstration purpose only. This is ideal but unrealistic, since it is usually not available).

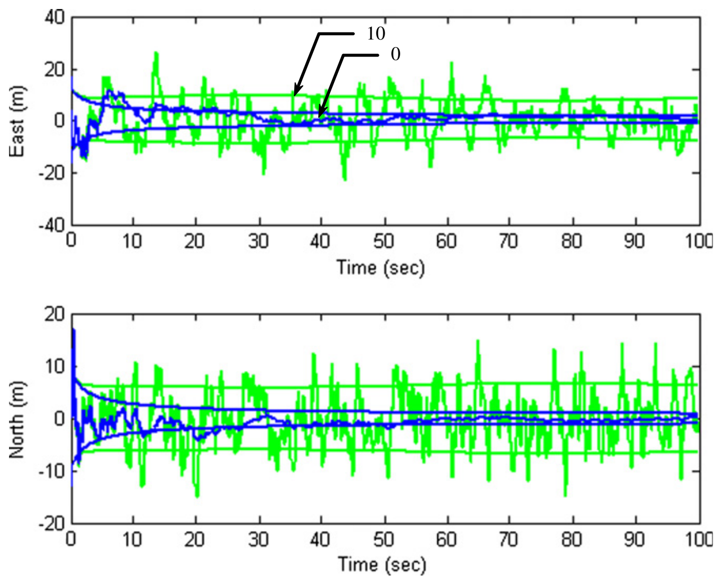

Fig. 5. Position estimation precision and the corresponding predicted $1-\sigma$ bound: small ($q_e = q_n = 0 (\mathrm{m/s^2})^2/(\mathrm{rad/s})$) versus large ($q_e = q_n = 10 (\mathrm{m/s^2})^2/(\mathrm{rad/s})$) PSD values.

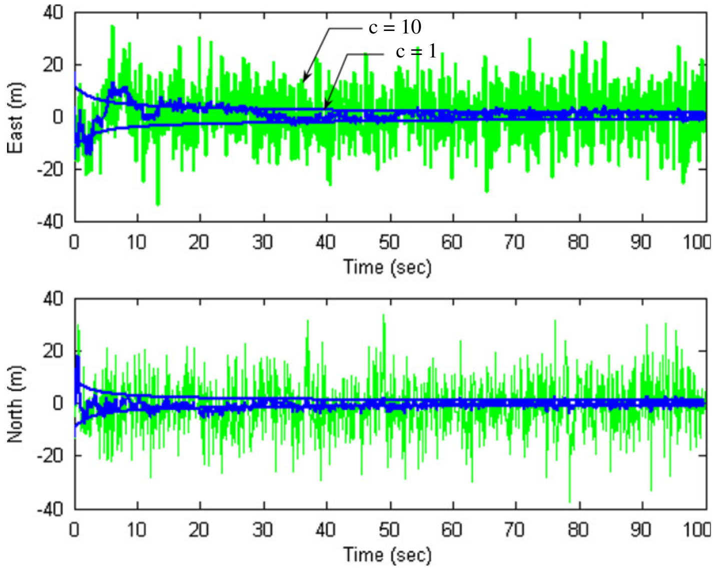

Fig. 6. Position estimation precision and the corresponding predicted $1-\sigma$ bound: small ($c=1$) versus large ($c=10$) random errors in reference trajectories (PSD: $q_e = q_n = 0(\mathrm{m/s^2})^2/(\mathrm{rad/s})$).

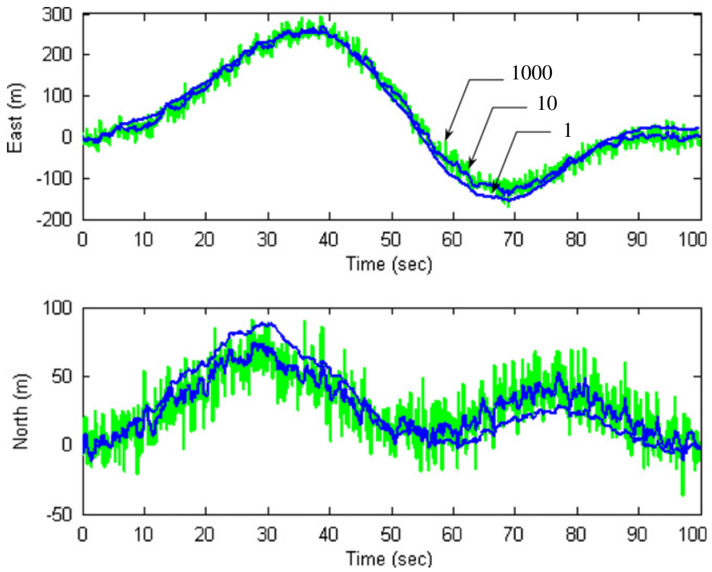

Fig. 7. Variation of the LKF estimation precision due to increase of process noise when reference trajectory is given by the actual trajectory distorted by bias errors (PSD: $q_e = q_n = 1000, 10, 1\ (\mathrm{m/s^2})^2/(\mathrm{rad/s})$).

Estimation precision can be improved in case the nominal (reference) trajectory is improved. For an exactly accurate reference trajectory, the zero dynamic process noise (i.e., PSD: $q_e = q_n = 0\ (\mathrm{m/s^2})^2/(\mathrm{rad/s})$) will be reasonable, leading the estimation error to zero. For the test case $q_e = q_n = 10\ (\mathrm{m/s^2})^2/(\mathrm{rad/s})$, the value is more than enough for convergence. As the PSD (or equivalently, $\mathbf{Q}_k$) increases, the result merely becomes noisy without noticeably change in the error mean. The confidence in the quality of reference trajectory is the core factor for determining the $\mathbf{Q}_k$. Fig. 5 shows the position estimation precision and the corresponding predicted $1-\sigma$ bound for small and large PSD values.

– *Case B:* Reference trajectory is given by the actual trajectory corrupted by zero mean random errors.

The PSD $q_e = q_n = 0\ (\mathrm{m/s^2})^2/(\mathrm{rad/s})$ and the scaling factor to the unity random errors $c = 10, 1$, respectively are used to control the magnitude of random errors in the nominal trajectory. Fig. 6 provides the position estimation precision and the corresponding predicted $1-\sigma$ bound for small vs. large random errors in reference trajectories with PSD: $q_e = q_n = 0\ (\mathrm{m/s^2})^2/(\mathrm{rad/s})$).

– *Case C:* Reference trajectory is given by the actual trajectory distorted by bias errors. For illustration, in this example the position at the initial epoch is used as the reference trajectory.

As the $\mathbf{Q}_k$ increases, the estimation precision decreases, and the result becomes more noisy and noisy. However, the bias error cannot be eliminated, even though a very

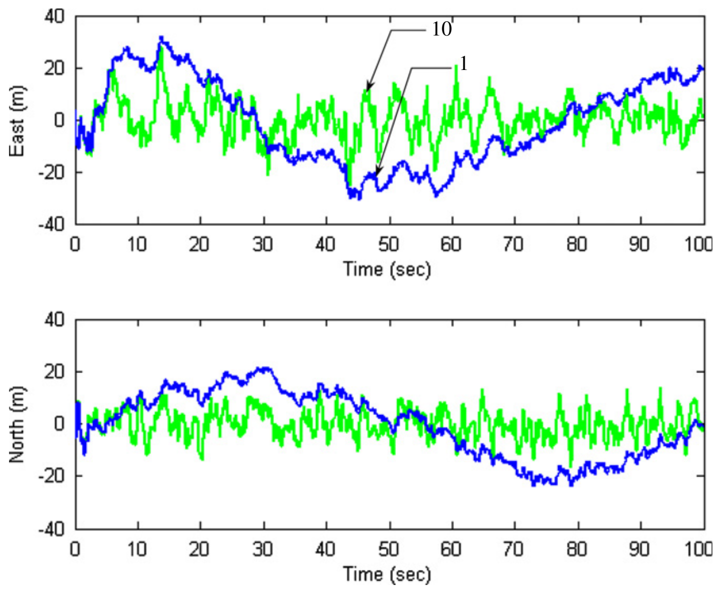

Fig. 8. Variation of the EKF estimation precision due to increase of process noise (PSD: $q_e = q_n = 10, 1\ (\mathrm{m/s^2})^2/(\mathrm{rad/s})$).

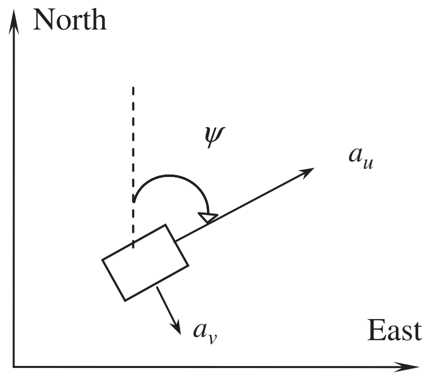

Fig. 9. Illustration of the two-dimensional inertial navigation.

large $\mathbf{Q}_k$ is applied. Fig. 7 shows the variation of the LKF estimation precision due to increase of process noise when reference trajectory is given by the actual trajectory distorted by bias errors. (PSD: $q_e = q_n = 1000, 10, 1\ (\mathrm{m/s^2})^2/(\mathrm{rad/s})$).

3.2. EKF performance

As discussed in the preceding section, the EKF is similar to a LKF except that the linearisation takes place about the filter's estimated trajectory, rather than a precomputed nominal trajectory. If the problem is sufficiently observable, the deviations between the estimated trajectory and the actual one should remain sufficiently small, and thus

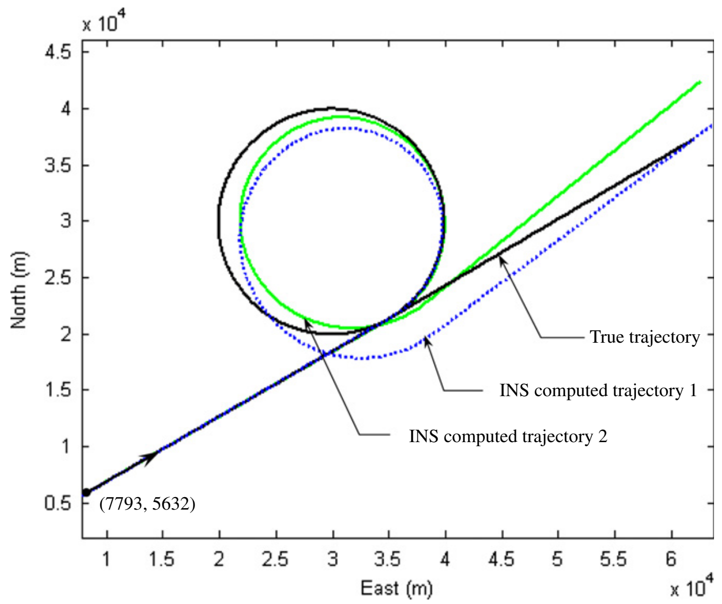

Fig. 10. Two of the possible INS computed trajectories as compared to the true trajectory.

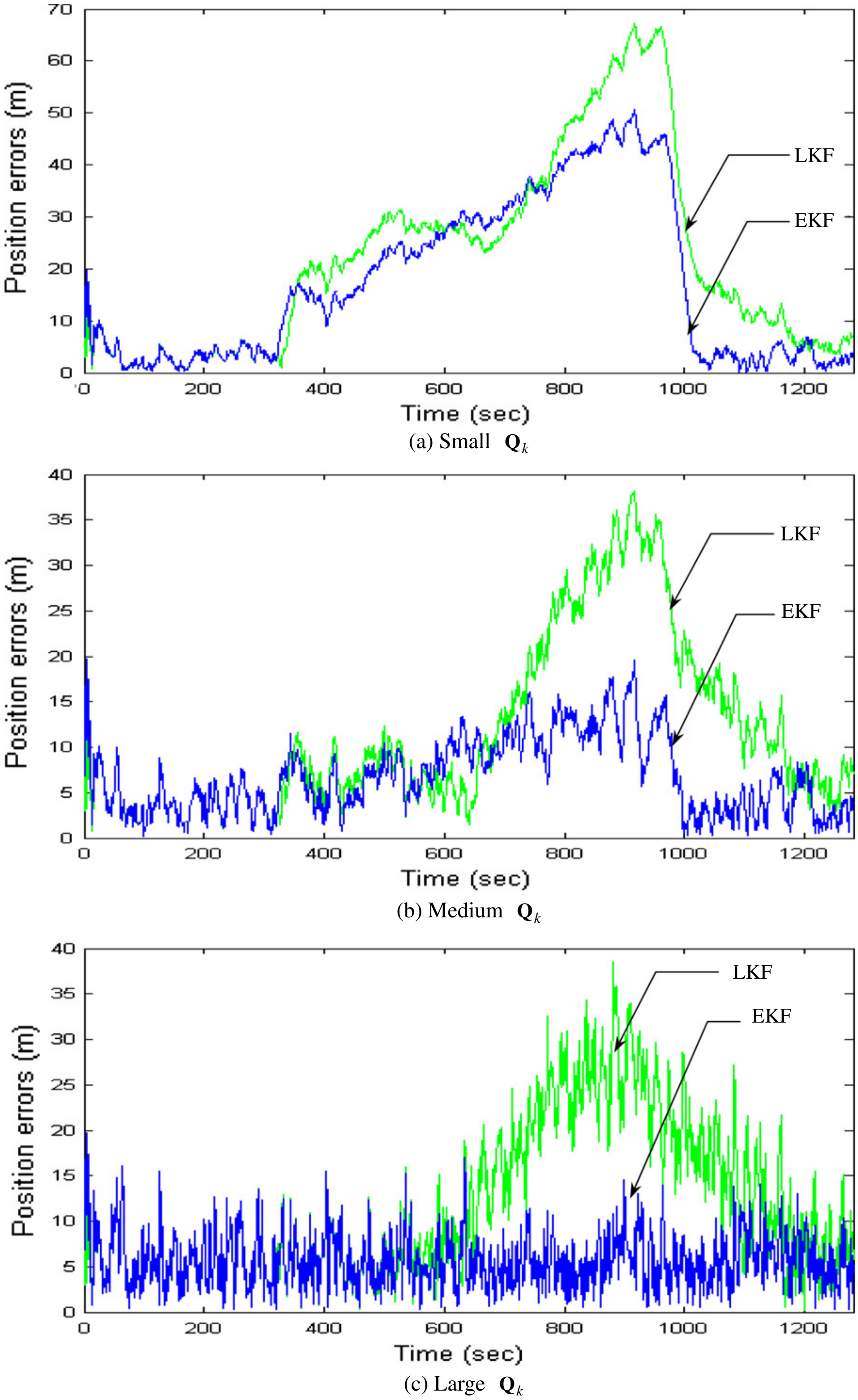

Fig. 11. Variation of the estimation precision due to increase of process noise for LKF and EKF – example for trajectory 1.

the linearisation assumption is valid. Fig. 8 shows the variation of the EKF estimation precision due to increase of process noise with PSD: $q_e = q_n = 10, 1(\mathrm{m/s^2})^2/(\mathrm{rad/s})$. The result confirms validity of the discussion.

A limitation in applying Kalman filter to real-world problems is that the *a priori* statistics of the stochastic errors in both dynamic process and measurement models are assumed to be available, which is difficult in practical application. The suboptimal configuration is typically based on a simplified error state dynamic/measurement model. One way to take them into account is to consider a nominal model affected by uncertainty.

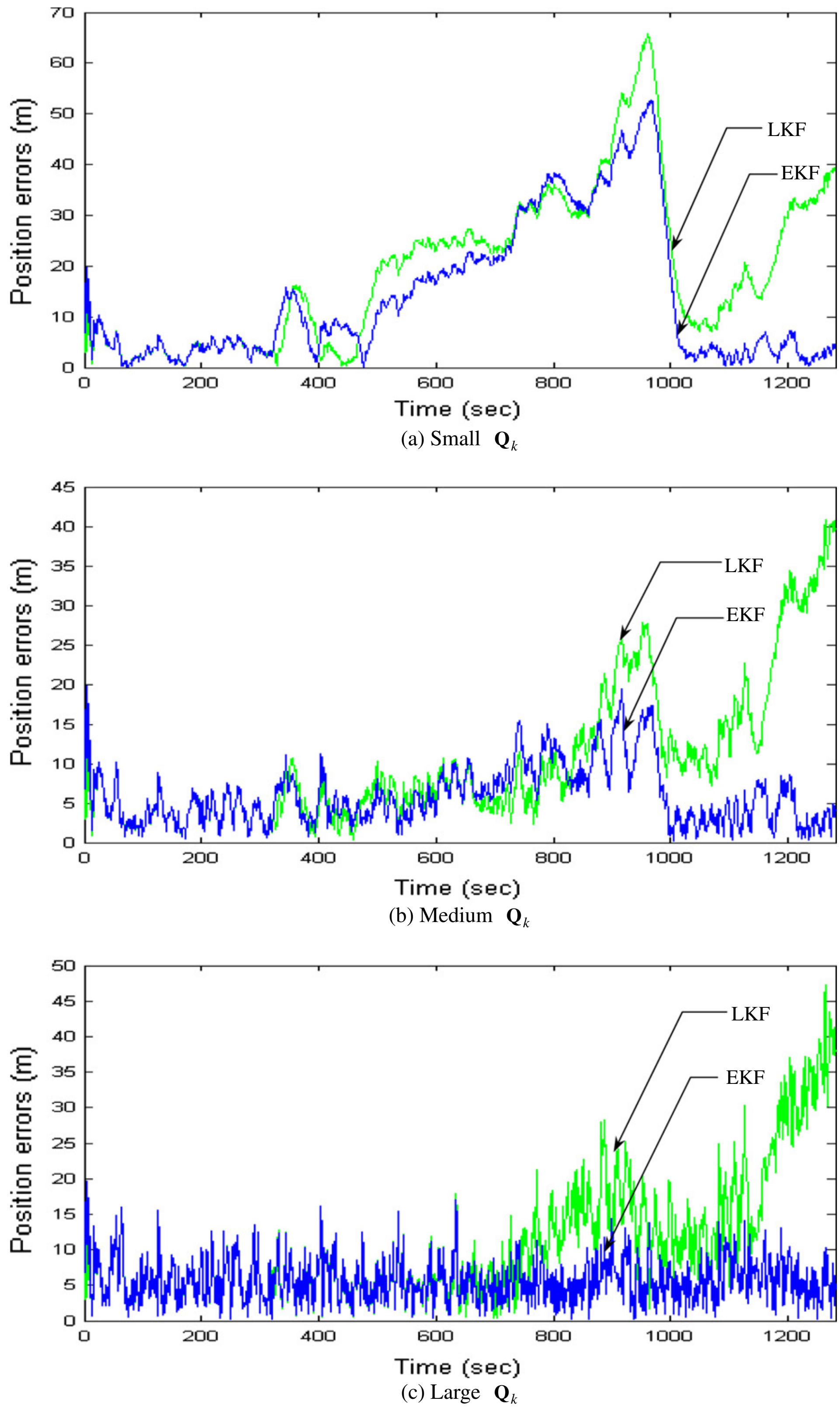

Fig. 12. Variation of the estimation precision due to increase of process noise for LKF and EKF – example for trajectory 2.

To fulfil the requirement of achieving the filter optimality, an adaptive Kalman filter (AKF) can be utilized as the noise-adaptive filter for tuning the noise covariance matrices and overcome the deficiency of Kalman filter. Adaptive filtering is based on dynamically adjusting the parameters of the filter. AKF's can be performed based on an on-line estimation of motion as well as the signal and noise statistics available data. It can be seen that AKF with covariance estimation based adaptation technique will be helpful for improving the precision in the EKF approach. However, this is not valid for the LKF approach.

4. Illustrative example – nominal trajectory is available

The second example employed for illustration is a case that the reference trajectory is available. One of the typical examples is the integrated navigation system in which KF fuses the INS (inertial navigation system) and DME data. Essentially, there are two aspects of integration: open loop (feedforward, equivalent to the LKF approach) versus closed loop (feedback, equivalent to the EKF approach). The differential equations describing the two-dimensional inertial navigation state are given by:

$$\begin{bmatrix} \dot{l}_e \\ \dot{v}_e \\ \dot{l}_n \\ \dot{v}_n \\ \dot{\psi} \end{bmatrix} = \begin{bmatrix} v_e \\ a_e \\ v_n \\ a_n \\ \omega_r \end{bmatrix} = \begin{bmatrix} v_e \\ \sin(\psi)a_u + \cos(\psi)a_v \\ v_n \\ \cos(\psi)a_u - \sin(\psi)a_v \\ \omega_r \end{bmatrix}$$

where $[a_u, a_v]$ are the measured accelerations in the body frame, ω_r is the measured yaw rate in the body frame, as shown in Fig. 9. The error model for INS is augmented by some sensor error states such as accelerometer biases and gyroscope drifts. Actually, there are several random errors associated with each inertial sensor. It is usually difficult to set a certain stochastic model for each inertial sensor that works efficiently at all environments and reflects the long-term behaviour of sensor errors. The difficulty of modelling the errors of INS raised the need for a model-less DME/INS integration technique. The following set of linearised equations is employed:

$$\begin{bmatrix} \delta\dot{l}_e \\ \delta\dot{v}_e \\ \delta\dot{l}_n \\ \delta\dot{v}_n \\ \delta\dot{\psi} \end{bmatrix} = \begin{bmatrix} 0 & 1 & 0 & 0 & 0 \\ 0 & 0 & 0 & 0 & 0 \\ 0 & 0 & 0 & 1 & 0 \\ 0 & 0 & 0 & 0 & 0 \\ 0 & 0 & 0 & 0 & 0 \end{bmatrix} \begin{bmatrix} \delta l_e \\ \delta v_e \\ \delta l_n \\ \delta v_n \\ \delta\psi \end{bmatrix} + \begin{bmatrix} 0 \\ u_e \\ 0 \\ u_n \\ u_\psi \end{bmatrix}$$

which will be utilized in the integration Kalman filter as the inertial error model for estimating the INS errors. The parameters δe and δn represent the east, and north position errors; δv_e and δv_n represent the east, and north velocity errors; and $\delta\psi$ represents yaw angle, respectively. The measurement in the indirect formulation is made up entirely of system errors and the filter and is almost independent of vehicle motions.

The measurement model is written as

$$\begin{bmatrix} \rho_1 \\ \rho_2 \\ \vdots \\ \rho_n \end{bmatrix} = \begin{bmatrix} \hat{\rho}_1 \\ \hat{\rho}_2 \\ \vdots \\ \hat{\rho}_n \end{bmatrix} + \begin{bmatrix} h_{11} & 0 & h_{13} & 0 & 0 \\ h_{21} & 0 & h_{23} & 0 & 0 \\ \vdots & \vdots & \vdots & \vdots & \vdots \\ h_{n1} & 0 & h_{n3} & 0 & 0 \end{bmatrix} \begin{bmatrix} \delta l_e \\ \delta v_e \\ \delta l_n \\ \delta v_n \\ \delta\psi \end{bmatrix} + \begin{bmatrix} v_1 \\ v_2 \\ \vdots \\ v_n \end{bmatrix}$$

Experiment was conducted on a simulated aircraft trajectory originating from the (7793, 5632) m location. The trajectory of the aircraft can be divided into two categories according to the dynamic characteristics. The aircraft was simulated to conduct constant-velocity straight-line during the two time intervals, 0–320 and 961–1281 all at 353.43 km/h speed (98.17 m/s). Furthermore, it conducted counter-clockwise circular motion with radius 10 km during 321–960 s, where higher dynamic is involved. Fig. 10 shows two of the possible unaided INS computed trajectories as compared to the true trajectory. The noise PSDs for accelerometers and gyroscopes used in the test case are as follows.

1. Small $\mathbf{Q}_k$: $q_e = q_n = 5e-4$; $q_\psi = 5e-5$.
2. Medium $\mathbf{Q}_k$: $q_e = q_n = 5e-3$; $q_\psi = 5e-4$.
3. Large $\mathbf{Q}_k$: $q_e = q_n = 500e-4$; $q_\psi = 500e-5$.

There is no specific reason to choose the numerical values.

There are three ranging sources coming from three DME stations, which are located at the following positions: DME1 = $(3e5, -1e4)$ m, DME2 = $(2.5e5, 2.5e5)$ m, DME3 = $(-1e4, 3e5)$ m. Furthermore, the noise characteristics is described by: $u_e \sim N(0, q_e)$; $u_n \sim N(0, q_n)$; and $u_\psi \sim N(0, q_\psi)$. These spectral amplitudes are used to establish the $\mathbf{Q}_k$ matrix.

Trajectory 1 has one, whereas Trajectory 2 has two regions where large errors may be induced due to large linearisation errors. Fig. 11 demonstrates variation of the estimation precision due to increase of process noise using the LKF and EKF for Trajectory 1. Fig. 12 demonstrates variation of the estimation precision due to increase of process noise using the LKF and EKF for Trajectory 2. The estimation performance provided for illustration is the 2-norm values of positioning errors.

What can be predicted is that even the adaptation algorithm is incorporated into the linearised Kalman filter for adapting $\mathbf{Q}_k$ matrix, precision improvement (possibly at the expense of precision degradation in the other regions) is still very limited due to large linearisation errors and are not likely to achieve acceptable precision. This implies that increase of the $\mathbf{Q}_k$ value will not be able to remedy the deviation and the AKF with $\mathbf{Q}_k$ adaptation will be little helpful in such type of problem. It is seen that, form Fig. 12, the errors will keep growing without bound after approximately 1200 s. One needs to either find better linearisation trajectories or choose better nonlinear models to fulfil the precision requirement.

5. Conclusions

This paper has pointed out several critical remarks which are useful for the designers in understanding, implementing and verifying two forms of nonlinear Kalman filter. An implementation-orientated approach is presented on several issues of considerable importance in engineering practice. Comparative study and critical remarks on the linearised and extended Kalman filters have been involved. It is hoped that the paper can serve as a tutorial to the readers for providing better understanding and therefore correctly implementing the two forms of nonlinear Kalman filter. Lessons learned from this paper include: linearisation of the nonlinear trajectories versus the system architectures, detailed implementation algorithms, and behaviour on the estimation precision, which are useful in designing an adequate suboptimal nonlinear Kalman filter.

Acknowledgements

This work was supported in part by the National Science Council of the Republic of China under Contract NSC 96-2221-E-19-007, NSC 97-2221-E-019-012 and NSC 98-2221-E-019-021-MY3. Valuable suggestions and detailed comments by the anonymous reviewers are gratefully acknowledged.

References

[1] Y. Bar-Shalom, X.R. Li, T. Kirubarajan, Estimation with Applications to Tracking and Navigation, John Wiley & Sons, Inc., 2001.
[2] K. Brammer, G. Karlsruhe, Kalman-Bucy Filters, Artech House, 1988.
[3] R. Brown, P. Hwang, Introduction to Random Signals and Applied Kalman Filtering, John Wiley & Sons, New York, 1997.
[4] A. Gelb, Applied Optimal Estimation, MIT Press, MA, 1974.
[5] M.S. Grewal, A.P. Andrews, Kalman Filtering, Theory and Practice Using MATLAB, second ed., John Wiley & Sons, Inc., 2001.
[6] S.P. Maybeck, Stochastic Models, Estimation, and Control, vol. I (1978), vol. II (1982), Academic Press.
[7] C. Hajiyev, Innovation approach based measurement error self-correction in dynamic systems, Measurement 39 (7) (2006) 585–593.
[8] Y.S. Shmaliy, O. Ibarra-Manzano, L. Arceo-Miquel, J. Munoz-Diaz, A thinning algorithm for GPS-based unbiased FIR estimation of a clock TIE model, Measurement 41 (5) (2008) 538–550.
[9] J. Ali, M. Ushaq, A consistent and robust Kalman filter design for in-motion alignment of inertial navigation system, Measurement 42 (4) (2009) 577–582.
[10] F. Wang, H. Jin, Design a mini-type marine attitude measurement system for self-propelled model trials, Measurement 42 (6) (2009) 954–962.
[11] R. Zhu, D. Sun, Z. Zhou, D. Wang, A linear fusion algorithm for attitude determination using low cost MEMS-based sensors, Measurement 40 (3) (2007) 322–328.
[12] S. Bogatin, K. Foppe, P. Wasmeier, T.A. Wunderlich, T. Schäfer, D. Kogoj, Evaluation of linear Kalman filter processing geodetic kinematic measurements, Measurement 41 (5) (2008) 561–578.
[13] K. Salahshoor, M. Mosallaei, M. Bayat, Centralized and decentralized process and sensor fault monitoring using data fusion based on adaptive extended Kalman filter algorithm, Measurement 41 (10) (2008) 1059–1076.
[14] L. Finkelstein, Measurement and instrumentation science – an analytical review, Measurement 14 (1) (1994) 3–14.
[15] F. Abdullah, L. Finkelstein, S.H. Khan, W.J. Hill, Modeling in measurement and instrumentation science – an overview, Measurement 14 (1) (1994) 41–53.
[16] R.Z. Morawski, Unified approach to measured reconstruction, IEEE Transactions on Instrumentation and measurement 43 (2) (1994) 226–231.
[17] K. H. Ruhm, Science and technology of measurement – a unified graphic-based approach, in: Proc. 10th IMEKO TC7 Int. Symposium, Saint-Petersburg, Russia, pp. 77–83.